

## IMPROVING BRAKE SQUEAL PROPENSITY PREDICTION BY MODEL UPDATING

Zhi Zhang, Sebastian Oberst, Jack J.R. Williams and Joseph C.S. Lai

Acoustics and Vibration Unit, School of Engineering and Information Technology,  
UNSW Canberra Australia, Canberra, Australia

Email: [zhi.zhang3@student.adfa.edu.au](mailto:zhi.zhang3@student.adfa.edu.au)

[s.oberst@adfa.edu.au](mailto:s.oberst@adfa.edu.au)

[jack.williams@student.adfa.edu.au](mailto:jack.williams@student.adfa.edu.au)

[j.lai@adfa.edu.au](mailto:j.lai@adfa.edu.au)

### Abstract

Brake squeal as a significant warranty-claim related costs problem to the automotive industry is difficult to model numerically and analyse because of inherent nonlinearities, uncertainties in material properties, contact and boundary conditions, and system complexity. Often, model components are linearised and not experimentally validated. Sophisticated contact or friction models as well as stiffness in joints are often not considered owing to difficulties in experimental validation. In this study, a full brake system is modally updated at the component level and then at the subassembly level (pad assembly alone, pad in bracket). Squeal prediction using the complex eigenvalue analysis on a finite element model of the system is compared to squeal results from a noise dynamometer test. The results are discussed with respect to further refinement of the modelling approach and improvements to brake squeal prediction.

### 1. Introduction

Brake squeal remains a major concern to the automotive industry owing to noise-related warranty claims and vehicle noise, vibration and harshness (NVH) performance reduction [1]. Brake squeal as a high-pitched audible sound above 1 kHz to 20 kHz is caused by friction-induced self-excited vibration. The prediction of its occurrence is difficult owing to (1) complexity [2, 3] and nonlinearity involved [4, 5], (2) many interacting mechanisms, such as mode-coupling [6], stick-slip [7], sprag-slip [8], instantaneous modes [9, 10], hammering [1], which can trigger and sustain squeal. The numerical methods for predicting brake squeal are the complex eigenvalue analysis (CEA) [11] and the transient time domain analysis [5, 12]. Using CEA to predict brake squeal in the frequency domain is industrial practice because it is more efficient than the time domain analysis. However, the CEA has been reported to under-predict [13] and over-predict [14] squeal generation. One likely reason is that the FE brake model does not accurately represent the realistic brake system and interactions among its components.

Parameter identification and model updating techniques can be applied to improve correlation between a numerical model and a physical system. Existing research of model updating applied to brake squeal can be categorised into different levels: components (rotor, pads, bracket, calliper) [15-17], subsystems (pad assembly, pads-in bracket, bracket in calliper) and a fully assembled system (all essential brake system components with or without wheel hub or car corner) [17]. Naturally, the parameter identification and model updating is expected to be more accurate at the assembly level as boundary conditions are fully considered. Tison et al. [17] update a full brake system but only consider

frequencies up to 3 kHz, only monitors the MAC in the full brake system and take only rotor modes into account without analysing the bracket, the pads or the calliper. Abu-Bakar conducted model updating to a full assembled brake system up to 9 kHz but unfortunately not many details are provided [15]. However, owing to the brake system's complexity i.e. in the boundary conditions (joints, backlashes, secondary reaction forces/contacts), various interacting parts, different materials, and owing to squeal frequencies ranging up to 20 kHz, it is important to conduct the model updating at the component, the subsystem and the assembly level to higher frequencies in a multi-stage updating framework. An updating process should include not only matching modes but also the response levels of test and numerical structures. Therefore, a sub-assembly consisting of a bracket, a pad lining and a backplate is considered in this study to identify the effect of the two abutment clips. The modelling of the abutment clips is rarely mentioned in the literature. It is either simply assumed that the bracket and the pad are linked together by springs with arbitrarily chosen stiffness the determination of the stiffness not detailed [16-19].

Following our previous work on the effect of model updating at the component level with the incorporation of a velocity-dependent friction law [16], the aim of this study is to evaluate how the squeal prediction by the CEA is affected by performing model updating to the sub-assembly of bracket, a single pad and backplate held together by abutment clips with stiffness values determined from experimental modal testing. Apart from updating the numerical brake model by a comparison of natural frequencies and mode shapes between experimental modal testing and FE results using the modal assurance criterion (MAC), experimentally determined modal damping and pressurisation area on both backplates are also considered and their effects on squeal prediction are investigated.

## 2. Numerical models

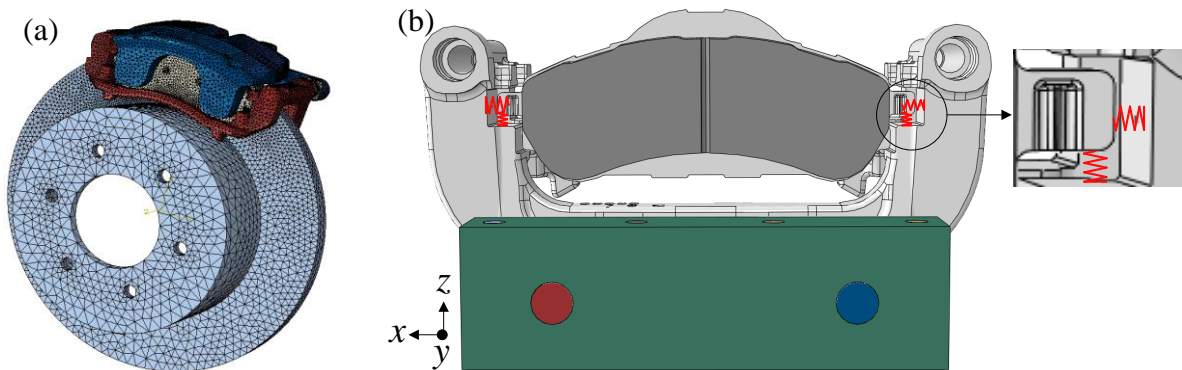


**Figure 1.** Finite element model of (a) a full brake system and (b) a bracket-pad subassembly.

**Table 1.** Numerical models A-G used for predicting brake squeal using CEA

Model	Mesh	Friction modelling	Material properties	Add. Damping	Springs simulating the abutment clips	Realistic pressurisation area
A	coarse	Amonton-Coulomb	Baseline	none	Baseline	none
B	<b>fine</b>	Amonton-Coulomb	Baseline	none	Baseline	none
C	fine	<b>Velocity-dependent</b>	Baseline	none	Baseline	none
D	fine	Velocity-dependent	<b>Updated</b>	none	Baseline	none
E	fine	Velocity-dependent	Updated	<b>Rayleigh</b>	Baseline	none
F	fine	Velocity-dependent	Updated	Rayleigh	<b>Updated</b>	none
G	fine	Velocity-dependent	Updated	Rayleigh	Updated	<b>Considered</b>

The full brake FE model modelled in ABAQUS 6.14-2 is depicted in Figure 1. The model is the same as that used by Williams et al. [16] and consists of a rotor, two pads, two backplates, a single piston calliper and a bracket (Figure 1(a)). Here, 12 springs are used to simulate the four abutment clips and connected via the backplate ears to the bracket, with three springs allocated to each clip in the  $x$ -,  $y$ -, and  $z$ - directions respectively (Figure 1(b)). Details of how the CEA is conducted, the extraction of model damping by fitting a Rayleigh damping curve and the contact interface modelling using different friction laws can be found in Williams et al. [16].

The evolution of the FE models from A to G is given in Table 1. The models A-E have been used in our previous work [16] and their instability prediction results will be presented again in section 4 to illustrate the successive enhancement in instability prediction induced by brake system model updating. For model E in Williams et al. [16], Rayleigh damping estimated from experimentally determined modal damping values is extracted by a least square curve fitting. However the squared 2-norm of the residual, which is used for evaluating the difference between the modal damping in the fitted curve with the tested modal damping, is sensitive to the initial guess of the parameters to extract. The least square curve fitting was performed with only one set of initial guess for each component [16]. Therefore curve fitting is repeated with 100 set of initial guesses in the presented paper to improve the quality of the Rayleigh damping identification. The results of the updated Rayleigh damping and the squared Euclidean distance of the residuals are listed in Table 2.

**Table 2.** The identified Rayleigh damping parameters and the squared 2-norm of the residual in the curve fitting

Components		$\alpha$	$\beta$	Square 2-norm residual
Rotor	Williams et al. [16]	118.20	$2.84 \times 10^{-9}$	$8.71 \times 10^{-5}$
	Updated	57.23	$7.89 \times 10^{-9}$	$4.13 \times 10^{-5}$
Calliper	Williams et al. [16]	493.02	$8.85 \times 10^{-8}$	$5.76 \times 10^{-4}$
	Updated	309.91	$1.78 \times 10^{-8}$	$2.93 \times 10^{-4}$
Pad lining	Williams et al. [16]	337.10	$8.88 \times 10^{-8}$	$4.31 \times 10^{-4}$
	Updated	365.55	$8.32 \times 10^{-8}$	$3.91 \times 10^{-4}$
Backplate	Williams et al. [16]	323.70	$-2.93 \times 10^{-9}$	$6.61 \times 10^{-4}$
	Updated	357.36	$-4.87 \times 10^{-9}$	$4.55 \times 10^{-4}$
Bracket	Williams et al. [16]	124.60	$5.13 \times 10^{-8}$	$1.20 \times 10^{-4}$
	Updated	39.60	$7.61 \times 10^{-8}$	$9.59 \times 10^{-5}$

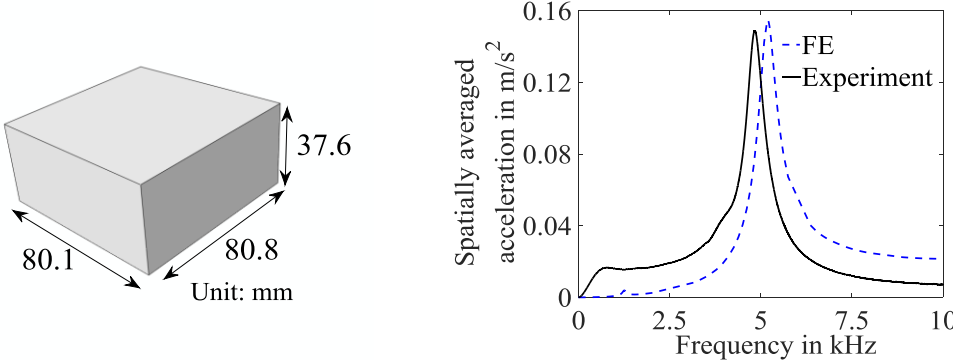
For model F, the stiffness of the springs simulating the abutment clips are determined experimentally for the first time in brake squeal studies. For model G, the pressure is applied on the nominal contacting surfaces between the piston-inner backplate and the calliper- outer backplate to approximate secondary reaction forces arising from the pressing of the calliper fingers on the outer pad.

### 3. Modal testing of pad – bracket sub-assembly and pressurisation on backplates

Frequency response function (FRF) were measured via modal testing using the following equipment in a frequency range of 50 Hz to 10 kHz: a Brüel and Kjær (B&K) type 4809 electro-dynamic shaker for exciting the components, a Polytec Scanning Laser Vibrometer (PSV-400) for obtaining the response signal, a Polytec OFV 5000 controller and the PSV 8.7 software for extracting and processing test data.

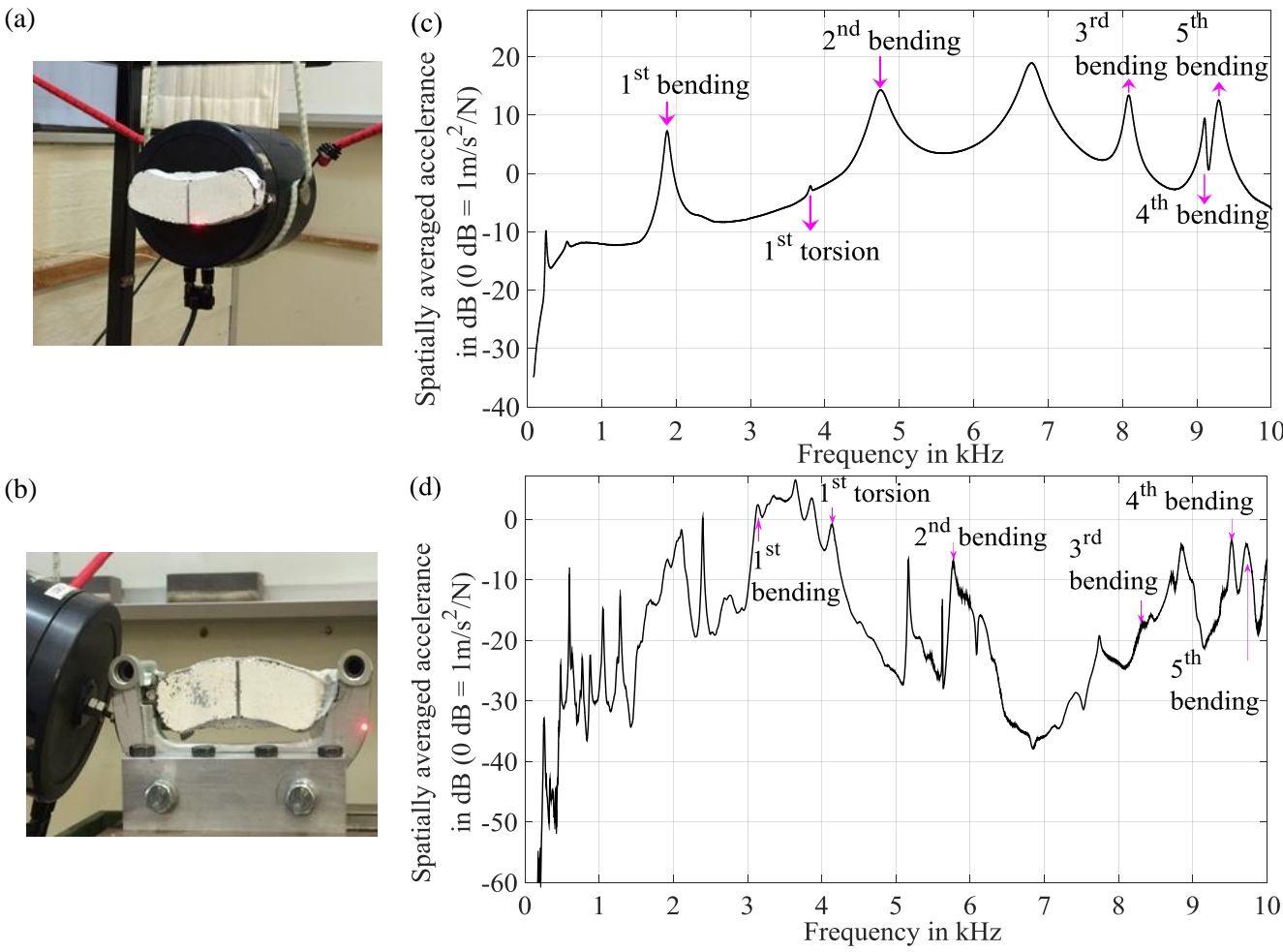
One important factor in measuring the FRF is ensuring that the force generated by the shaker is correctly acquired because it serves as the input for the FRF calculation. For the purpose of control and for further studies, an aluminium block of 0.632 kg shown in Figure 2(a) is used. The force generated by the shaker is indirectly obtained by multiplying the homogenously distributed mass with its the spatial averaged acceleration. The measured acceleration of the block in Figure 2 (b) shows only one peak of  $0.149 \text{ m/s}^2$  in the frequency range up to 4 kHz. The force generated by the shaker is 0.095 N so that the setting of our data analysis system can be adjusted accordingly to allow testing of a structure without using a force transducer (e.g. for very light structures such as the damping shim alone).For

validation of the identified force, a forced response analysis is performed to the FE block model with a force of 0.095 N at the excitation point and experimentally extracted modal damping being applied. The frequency of the tested and simulated peak is different. This could be due to the discrepancy of the boundary condition between the measurement (a hole was drilled on the back side for linking the shaker) and simulation (all the DOF of the hole is frozen in FE). The simulated spatially averaged acceleration is shown in Figure 2 (b) and its peak is close to the one measured which suggests the identified force is acceptable.



**Figure 2.** The model of the aluminium block (a) and the measured and calculated (with identified shaker force being applied) spatially averaged acceleration

**3.1 Modal testing of pad in free-free and assembled conditions**

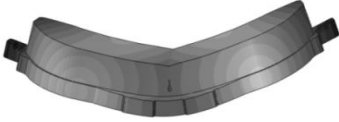
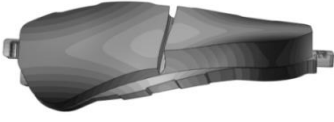
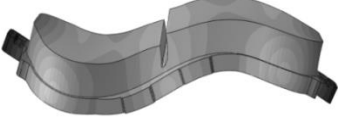


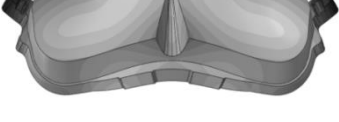


**Figure 3.** Modal testing of a pad (a) setup in free-free condition; (b) spatially averaged accerlence in free-free condition; (c) setup in assembled condition; (d) spatially averaged accerlence in assembled

The modal testing was conducted with the pad-assembly (lining plus backplate) under two measurement conditions in order to measure the frequency shift of identified pad modes: free-free and one pad assembled to the bracket using two abutment clips. The objective of doing two testings is to

measure the frequency shift of each mode. The natural frequency of a mode in free-free condition is expected to shift to a higher frequency in the assembled condition because of the effect of the abutment clips. Then the stiffness of the abutment clips can be extracted by relating it to the measured frequency shift. The setup of the modal testing of a pad in free-free and assembled condition is shown in Figure 3(a) and (b), respectively. The pad was suspended by shock cords to approximate the free-free condition. For the assembled condition, the pad was first set in the bracket using the abutment clip then the bracket was screwed to an adapter mounted on a milling machine. The scanning surface was sprayed with an inert white powder to reduce the speckle noise found with lasers on highly reflective surfaces. The 365 scanning points and the averaged accelerance over these scanning points for the two conditions is shown in Figure 3 (c) and (d), respectively. It is shown in Figure 3 (b) that the pad has 6 modes with well-correlated FE mode shapes, as indicated by the MAC (Modal Assurance Criterion) in Table 1. It is noted in Figure 3 (b) that there is a peak next to the 2<sup>nd</sup> bending mode not marked as a mode because it does not appear in a modal testing excited by a hammer in free-free condition. It is shown in Figure 3 (d) that many more peaks appear in the assembled condition. As expected the bracket modes are mixed with those of the pad. Those mixed modes which are (1) dominated by a pad's mode and which (2) correlate well with the 6 modes measured in the free-free condition need to be identified. The satisfactory modes (with reasonable MAC in the cross comparison of the modes in free-free with assembled conditions) are found and indicated by arrows in Figure 3 (d). The resonance frequency of the 6 pad's mode in both measurement conditions are listed in Table 3 and the frequency shift is calculated and shown in Table 4.

**Table 3.** Correlation of FE with modal testing results of a pad-backplate assembly

Mode	Measurement condition	Measured frequency (Hz)	FE mode shapes	MAC (FE-test)
1 <sup>st</sup> bending	Free-free	1875.5		97.8%
	Assembled	3132.3		77.8%
1 <sup>st</sup> torsion	Free-free	3813.8		89.8%
	Assembled	4151.7		88.0%
2 <sup>nd</sup> bending	Free-free	4740.0		71.9%
	Assembled	5760.7		72.7%
3 <sup>rd</sup> bending	Free-free	8082.6		98.1%
	Assembled	8338.2		88.4%
4 <sup>th</sup> bending	Free-free	9109.6		96.0%
	Assembled	9525.4		92.2%
5 <sup>th</sup> bending	Free-free	9286.7		95.3%
	Assembled	9714.5		83.3%

**Table 4.** Identification of abutment clip stiffness

Mode	DOF participation (%)			Frequency shift from free-free to assembled (Hz)	Modal mass (kg)	Stiffness of the abutment clip ( $10^5$ N/m)			
	x	y	z			x	y	z	Total
1 <sup>st</sup> bending	7.6	12.3	80.1	1256.8	0.0516	0.1234	0.1999	1.3020	1.6253
1 <sup>st</sup> torsion	18.9	18.4	62.7	337.9	0.0623	0.1590	0.1542	0.5250	0.8381
2 <sup>nd</sup> bending	18.5	23.7	57.9	1020.7	0.0326	0.3229	0.4133	1.0111	1.7473
3 <sup>rd</sup> bending	8.5	54.6	36.9	255.6	0.0623	0.1114	0.7130	0.4824	1.3068
4 <sup>th</sup> bending	7.5	31.9	60.6	415.8	0.0366	0.1072	0.4537	0.8589	1.4197
5 <sup>th</sup> bending	9.5	31.1	59.4	427.8	0.0468	0.1804	0.5920	1.1303	1.9026

Next the stiffness of the abutment clips is determined. The modal frequency in the free-free condition ( $f_{fi}$ ,  $i = 1-6$ ) and in the assembled condition ( $f_{ai}$ ) can be calculated from

$$f_{fi} = \sqrt{\frac{k_i}{m_i}}, \quad f_{ai} = \sqrt{\frac{k_i + 2k_i^a}{m_i}}, \quad (1)$$

where  $k_i$ ,  $m_i$ ,  $k_i^a$  denote respectively the modal stiffness, the modal mass and the stiffness of the abutment clip for mode  $i$ . From Eq. (1),  $k_i^a$  can be determined by

$$k_i^a = 0.5m_i \cdot (f_{ai}^2 - f_{fi}^2), \quad (2)$$

with the modal mass  $m_i$  being obtained from ABAQUS.

The value of the calculated stiffness of the abutment clip is given in Table 2, in which the ‘‘Total’’ stiffness is  $k_i^a$  and it is decomposed into 3 components (springs parallel to  $x$ ,  $y$ ,  $z$  direction) by multiplying  $k_i^a$  with the DOF participation (given by ABAQUS). The average of the components of  $k_i^a$  is taken as the stiffness of the three springs parallel to the  $x$ -,  $y$ -, and  $z$ - directions connecting the bracket with one pad of the FE model shown in Figure 1(b).

### 3.2 Pressurisation area on the backplates

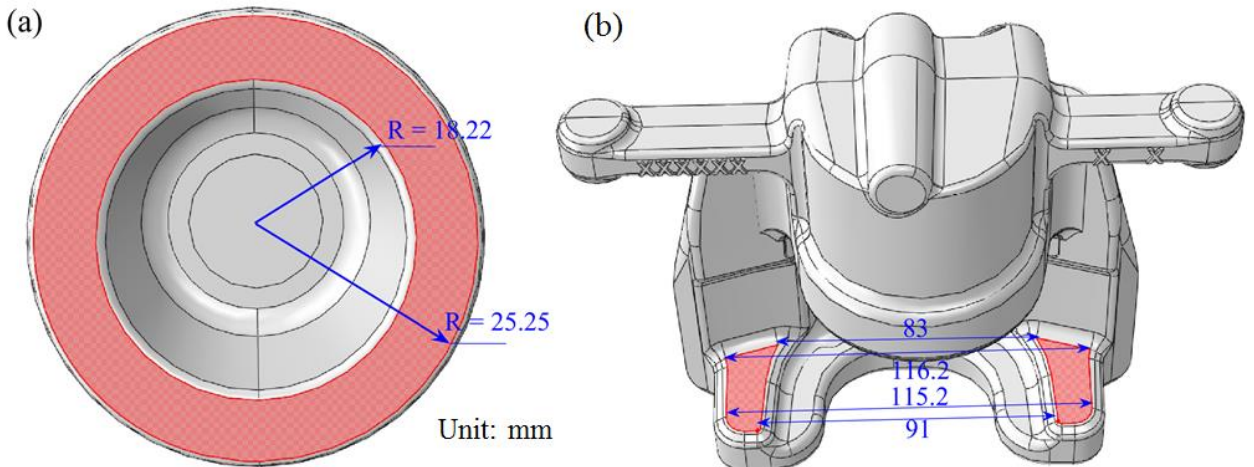


**Figure 4** Areas of pressure application (a) the piston annulus acting on the inner backplate, and (b) the fingers of the calliper acting on the outer backplate

In our previous work [16], the pressurisation area on the two backplates imprecise. Here, the area of the pressure applied by the piston on the inner backplate and by the fingers of the calliper on the outer backplate in the FE model is highlighted by the red area as shown in Figure 4 (a). The magnitude of the applied pressure in FE model is 12.8 bar [16].

#### 4. Comparison of instability prediction and the noise dynamometer test

Squeal dynamometer tests were conducted in a computer-controlled industrial noise dynamometer and the brake noise with sound pressure level (SPL) larger than 70 dB was recorded as detailed in Ref.[16]. Figure 5 shows the comparison of various instability predictions with the squeal dynamometer test results. The results indicate that (a) compared to the un-damped models (A-D), the new models E – G produces fewer unstable modes; (b) two squeal events with frequencies of 4850 Hz and 13800 Hz are predicted by all the models suggesting these unstable modes are robust and insensitive to the model used; (c) one squeal event at 6675 Hz is only accurately predicted by model G; and (d) the CEA still over-predicts the number of modes (10 kHz and 16 kHz) and does not detect the three instabilities at 2kHz, 9 kHz and 11.9 kHz.

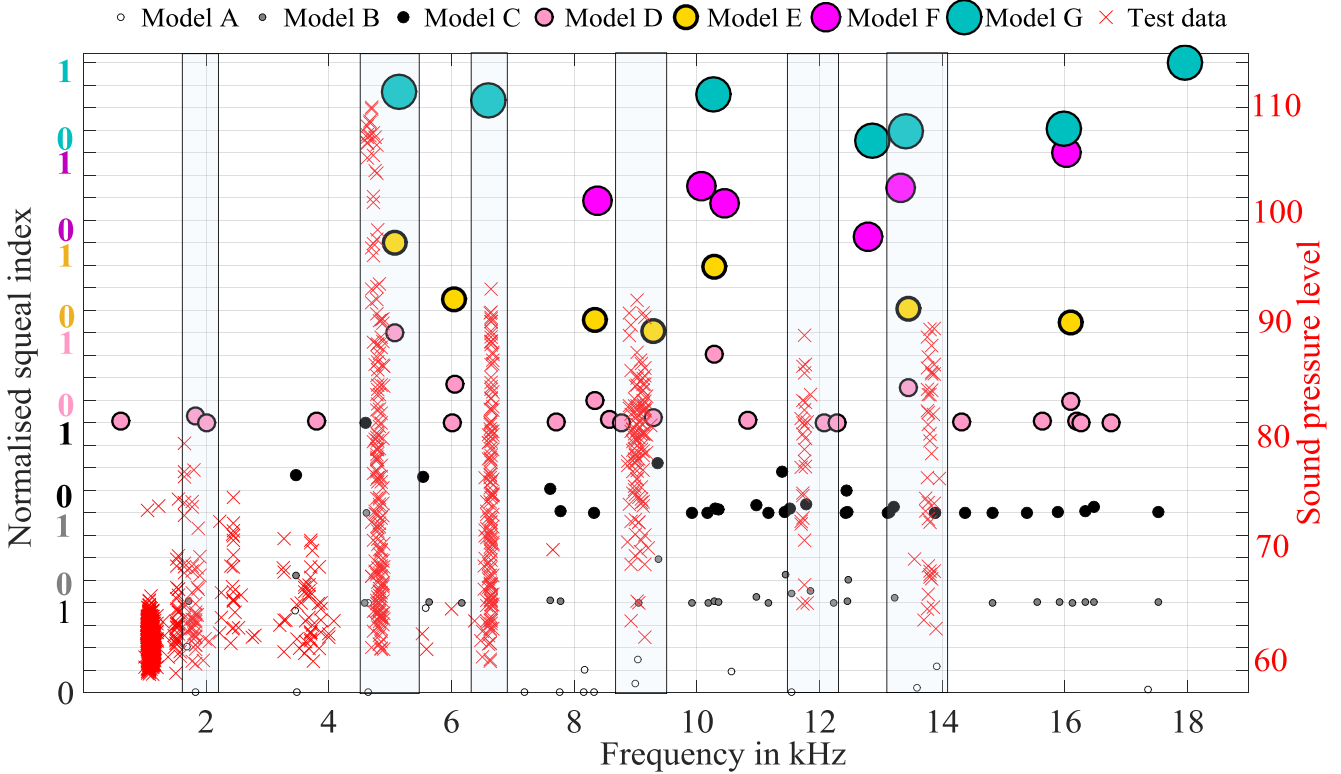


**Figure 5.** Comparison of instability predictions with brake dynamometer tests

#### 5. Conclusion

The influence of improving the modelling of a full FE brake model by performing model updating on a bracket-pad subassembly and defining a more realistic pressurisation area on its squeal prediction using the complex eigenvalue analysis is investigated. The FE model is improved by applying Rayleigh damping, updated abutment clip stiffness not previously attempted in brake squeal studies, and realistic pressurisation area on the inner and outer pad. The results show that as expected, the incorporation of Rayleigh damping eliminates many unstable modes. More importantly the stiffness of the springs simulating the abutment clips is important in predicting unstable vibration modes which result in squeal and the pressurised area also has a significant influence on the instability prediction. The comparison instability predictions with experimental noise dynamometer tests show that the model G with both updated abutment clip stiffness and pressurised area predicts most squealing events with reduced over prediction by employing Rayleigh damping. However, not all squealing events are predicted and there are instabilities that do not result in squeal. Hence, for better instability prediction, the model has to be further refined by conducting model updating for the fully assembled brake system.

## Acknowledgements

The first author is grateful to be a recipient of the travel award provided by the Australian Acoustical Society to attend the Acoustics 2015 conference in Hunter Valley, and acknowledges receipt of a UNSW University College Postgraduate Research Scholarship for the pursuit of this study. This research was undertaken with the assistance of resources provided at the National Computational Infrastructure, Australia. The provision of brake squeal dynamometer test data by Chassis Brakes International is gratefully acknowledged.

## References

- [1] Kinkaid, N.M, O'Reilly, O.M., Papadopoulos, P., "Automotive disc brake squeal", *Journal of Sound and Vibration*, **267**, 105-166, (2003).
- [2] Oberst, S., Lai, J.C.S., "Statistical analysis of brake squeal noise", *Journal of Sound and Vibration*, **330**, 2978-2994, (2011).
- [3] Oberst, S., Lai, J.C.S. "A statistical approach to estimate the Lyapunov spectrum in disc brake squeal", *Journal of Sound and Vibration*, **334**, 120-135, (2015).
- [4] Oberst, S., Lai, J.C.S. "Chaos in brake squeal noise", *Journal of Sound and Vibration*, **330**, 955-975, (2011)
- [5] Oberst, S., Lai, J.C.S. "Nonlinear transient and chaotic interactions in disc brake squeal", *Journal of Sound and Vibration*, **342**, 272-289, (2015)
- [6] Hoffmann, N., Fischer M., Allgaier R., Gaul L. "A minimal model for studying properties of the mode-coupling type instability in friction induced oscillations", *Mechanics Research Communications*, **29**, 197-205, (2002).
- [7] Behrendt, J., Weiss, C., Hoffmann N. "A numerical study on stick-slip motion of a brake pad in steady sliding", *Journal of Sound and Vibration*, **330**, 636-651, (2011).
- [8] Hoffmann, N., Gaul L. "A sufficient criterion for the onset of sprag-slip oscillations", *Archive of Applied Mechanics (Ingenieur Archiv)*, **73**, 650-660, (2004).
- [9] Oberst, S., Lai, J.C.S. "Pad-mode-induced instantaneous mode instability for simple models of brake systems", *Mechanical Systems and Signal Processing*, **63**, 490-505, (2015).
- [10] Oberst, S., Lai, J.C.S. "Squeal noise in simple numerical brake models", *Journal of Sound and Vibration*, **352**, 129-141, (2015).
- [11] Oberst S., Lai, J.C.S., Marburg, S., "Guidelines for numerical vibration and acoustic analysis of disc brake squeal using simple models of brake systems", *Journal of Sound and Vibration*, **332**, 2284-2299, (2013).
- [12] Sinou, J.J. "Transient non-linear dynamic analysis of automotive disc brake squeal – On the need to consider both stability and non-linear analysis", *Mechanics Research Communications*, **37**, 96-105, (2010).
- [13] Zhang, Z., Oberst, S., Lai, J.C. "Instability prediction of brake squeal by nonlinear stability analysis", *Proceedings of Internoise 2014*, Melbourne, Victoria, Australia, 16-19 November, 2014, pp 1-7.
- [14] Bajer, A., Belsky, V., Kung, S.W. "The influence of friction-induced damping and nonlinear effects on brake squeal analysis", *SAE Technical Paper*, 2004-01-2794.
- [15] AbuBakar, A.R., Ouyang, H. "A prediction methodology of disk brake squeal using complex eigenvalue analysis", *International Journal of Vehicle Design*, **46**, 416-435, (2008).
- [16] Williams, J., Zhang, Z., Oberst, S., Lai, J.C.S., "Model updating of brake components' influence on instability predictions", *International congress on sound and vibration*. Florence, Italy, 12-16 July, 2015, pp 1-8.
- [17] Tison, T., Heussaff, A., Massa, F., Turpin, I., Nunes, R.F. "Improvement in the predictivity of squeal simulations: Uncertainty and robustness", *Journal of Sound and Vibration*, **333**, 3394-3412, (2014).
- [18] Dai, Y., Lim, T.C. "Suppression of brake squeal noise applying finite element brake and pad model enhanced by spectral-based assurance criteria", *Applied Acoustics*, **69**, 196-214, (2008).
- [19] Fritz, G., Sinou, J.J., Duffal, J.M. and Jezequel, L. "Investigation of the relationship between damping and mode-coupling patterns in case of brake squeal", *Journal of Sound and Vibration*, **307**, 591-609, (2007).